Adipose tissue B2 cells promote insulin resistance through leukotriene LTB4/LTB4R1 signaling

Wei Ying,[1,2] Joshua Wollam,[1] Jachelle M. Ofrecio,[1] Gautam Bandyopadhyay,[1] Dalila El Ouarrat,[1] Yun Sok Lee,[1] Da Young Oh,[1] Pingping Li,[3] Olivia Osborn,[1] and Jerrold M. Olefsky[1]

[1]Division of Endocrinology and Metabolism, Department of Medicine, UCSD, La Jolla, California, USA. [2]Research Center for Translational Medicine, East Hospital, Tongji University School of Medicine, Shanghai, China. [3]State Key Laboratory of Bioactive Substance and Function of Natural Medicines, Institute of Materia Medica, Peking Union Medical College and Chinese Academy of Medical Sciences, Beijing, China.

Tissue inflammation is a key component of obesity-induced insulin resistance, with a variety of immune cell types accumulating in adipose tissue. Here, we have demonstrated increased numbers of B2 lymphocytes in obese adipose tissue and have shown that high-fat diet–induced (HFD-induced) insulin resistance is mitigated in B cell-deficient (B^{null}) mice. Adoptive transfer of adipose tissue B2 cells (ATB2) from wild-type HFD donor mice into HFD B^{null} recipients completely restored the effect of HFD to induce insulin resistance. Recruitment and activation of ATB2 cells was mediated by signaling through the chemokine leukotriene B4 (LTB4) and its receptor LTB4R1. Furthermore, the adverse effects of ATB2 cells on glucose homeostasis were partially dependent upon T cells and macrophages. These results demonstrate the importance of ATB2 cells in obesity-induced insulin resistance and suggest that inhibition of the LTB4/LTB4R1 axis might be a useful approach for developing insulin-sensitizing therapeutics.

Introduction

The global epidemic of type 2 diabetes is increasing at an alarming rate in both Westernized and developing countries. In the United States alone, it is estimated that there are at least 30 million people with this disease (1, 2). Metabolic syndrome is 2 to 3 times more prevalent than type 2 diabetes and is usually the precursor state for this disease (3), indicating that this type 2 diabetes epidemic will not abate in the near future. Insulin resistance is a key etiologic feature of the metabolic syndrome and type 2 diabetes, and obesity is far and away the most common cause of insulin resistance in humans (4–6). There is a well-known parallel global epidemic of obesity, and the great majority of type 2 diabetic patients are obese (1, 2). Therefore, it seems logical to conclude that the obesity epidemic is the underlying driver of the type 2 diabetes epidemic.

It is well established that chronic tissue inflammation, particularly in adipose tissue, is a characteristic feature of obesity in both rodents and humans, and many studies have demonstrated that this chronic inflammatory state is a key contributor to decreased insulin sensitivity (7–11). Macrophages and different T cell subtypes have been particularly well studied, and several secretory factors that can cause decreased insulin sensitivity have already been identified (12–18). Less is known about the role of B cells in this process, but reports demonstrate that an increased composition of B cells is also a feature of adipose tissue in obesity (19–21). In addition, genetic depletion of B cells partially prevents the effects of HFD in inducing adipose tissue inflammation and insulin resistance (19–21). Thus, B cells can modulate adipose tissue function in obesity; however, the operative B cell subtypes and the mechanisms for recruitment and activation of these cells are poorly understood.

Leukotriene B4 (LTB4) is an arachidonic acid–derived proinflammatory lipid mediator that is produced through the sequential activities of 5-lipoxygenase, 5-lipoxygenase–activating protein, and leukotriene A_4 hydrolase (22, 23). LTB4 binds with high affinity to its G protein–coupled receptor, LTB4R1 (also known as BLT1) (24). After specifically binding to LTB4R1, LTB4 exerts robust effects to promote leukocyte infiltration into various tissues and regulates proinflammatory cytokine production (25–29). Previous studies have demonstrated effects of the LTB4/LTB4R1 axis on recruitment and activation of macrophages in the context of obesity (30–34). In addition, LTB4 can exert direct effects on hepatocytes and myocytes to impair insulin signaling (34).

In the current study, we report that adipose tissue B2 (ATB2) cells accumulate in obesity and contribute to insulin resistance and glucose intolerance. These effects are partially dependent on T cells and macrophages. Finally, depletion of LTB4R1 prevents B2 cell recruitment into visceral fat depots, mitigating the contribution of B2 cells to the pathogenesis of obesity-induced adipose tissue inflammation and insulin resistance.

Results

Expression pattern of LTB4R1 in tissue-resident B cells. B cell recruitment to adipose tissue is increased in obesity. Thus, while accounting for approximately 10% of stromal vascular cells (SVCs) in lean adipose tissues, B cells can compose approximately 20% of SVCs in obesity (Figure 1A). Most of these recruited adipose tissue B cells exhibit a B2 cell phenotype ($CD19^+CD5^-$, Figure 1A). Our previous data also showed increased ATB2 cell

Conflict of interest: The authors have declared that no conflict of interest exists.
Submitted: August 26, 2016; **Accepted:** December 15, 2016.
Reference information: *J Clin Invest.* 2017;127(3):1019–1030.
https://doi.org/10.1172/JCI90350.

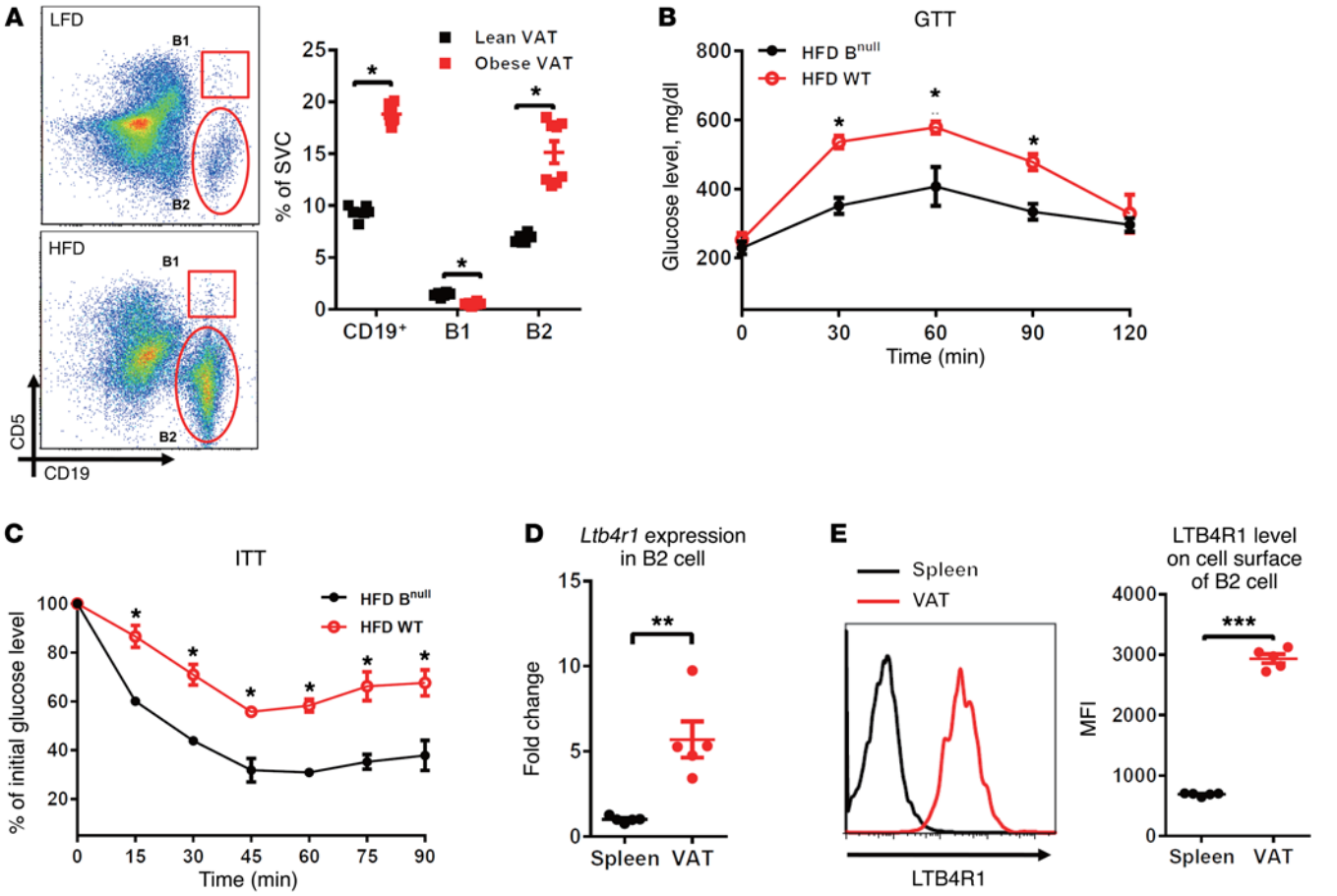

Figure 1. LTB4R1 expression pattern in various tissue-resident B2 cells. (**A**) The population of the B cell subsets B1 cell ($CD19^+CD5^+$) and B2 cell ($CD19^+CD5^-$) in VAT of LFD- and HFD-fed WT mice, shown quantitatively to the right. (**B** and **C**) GTTs and ITTs of HFD-fed B^{null} and WT mice. (**D** and **E**) Gene expression of *Ltb4r1* and its protein level in spleen and VAT B2 cells of HFD-fed WT mice. Data are presented as mean ± SEM. $n = 6$ per group (**A**–**E**). $^*P < 0.05$, $^{**}P < 0.01$, $^{***}P < 0.001$, Student's *t* test (**A**, **D**, **E**); 1-way ANOVA with Bonferroni's post test (**B** and **C**).

content in human obesity. Thus, in a study of insulin-resistant obese (BMI 35.6 ± 1.4 kg/m^2) and lean subjects (BMI 24.6 ± 0.8 kg/m^2), the expression level of the human B2 cell marker B220 (protein tyrosine phosphatase receptor type C [*PTPRC*]), as measured by Affymetrix Human Genome microarrays, was 2.7-fold elevated in obese adipose tissue (35).

The B cell–deficient (B^{null}) mouse lacks B cells due to a mutation preventing expression of *Ighm* (36). Importantly, depletion of B cells improves glucose tolerance and insulin sensitivity in high-fat diet (HFD)/obese mice, indicating a critical role for recruited B cells in obesity-related metabolic disorders (Figure 1, B and C). The chemokine LTB4 and its receptor LTB4R1 are known to mediate macrophage recruitment to obese adipose tissue, which promotes insulin resistance (31, 34). To examine the expression pattern of LTB4R1 in distinct tissue B2 cells, we isolated B2 cells from spleen and the visceral adipose tissue (VAT) of obese WT mice. Compared with naive splenic B2 cells, the recruited VAT B2 cells exhibited substantially greater *Ltb4r1* gene expression (Figure 1D). Our flow cytometry analyses confirmed increased LTB4R1 protein expression on the cell surface of VAT-resident B2 cells compared with splenic B2 cells (Figure 1E). We also detected expression of LTB4R1 in B1 cells ($CD19^+CD5^+$); however, there was no difference in LTB4R1 levels between splenic and adipose-resident B1 cells (Supplemental Figure 1; supplemental material available online with this article; doi:10.1172/JCI90350DS1). Based on these findings, we have explored the effect of the LTB4/LTB4R1 axis on the activity and function of B2 cells in the context of obesity.

The LTB4/LTB4R1 axis promotes B2 cell chemotaxis. Given the robust expression of LTB4R1 on recruited B2 cells, we next examined whether the LTB4/LTB4R1 axis plays a role in B2 cell chemotaxis. In in vitro Transwell chemotaxis assays (34, 37), LTB4 led to a dose-responsive increase in splenic B2 cell migration (Figure 2A), and these effects were absent using splenic B2 cells isolated from *Ltb4r1* knockout (hereafter referred to as *Ltb4r1*KO) mice. In addition, cotreatment with the LTB4R1 inhibitor (CP-105696) completely blocked LTB4-induced B2 cell chemotaxis (Figure 2B).

We measured adipose tissue LTB4 levels and found a 2- to 3-fold increase in VAT from HFD mice, compared with lean low-fat diet–fed (LFD-fed) mice (Figure 2C). Interestingly, when we isolated primary adipocytes and SVCs from VAT of HFD WT mice, we found that adipocytes secreted a substantial amount of LTB4, while SVCs secreted much less (Supplemental Figure 2).

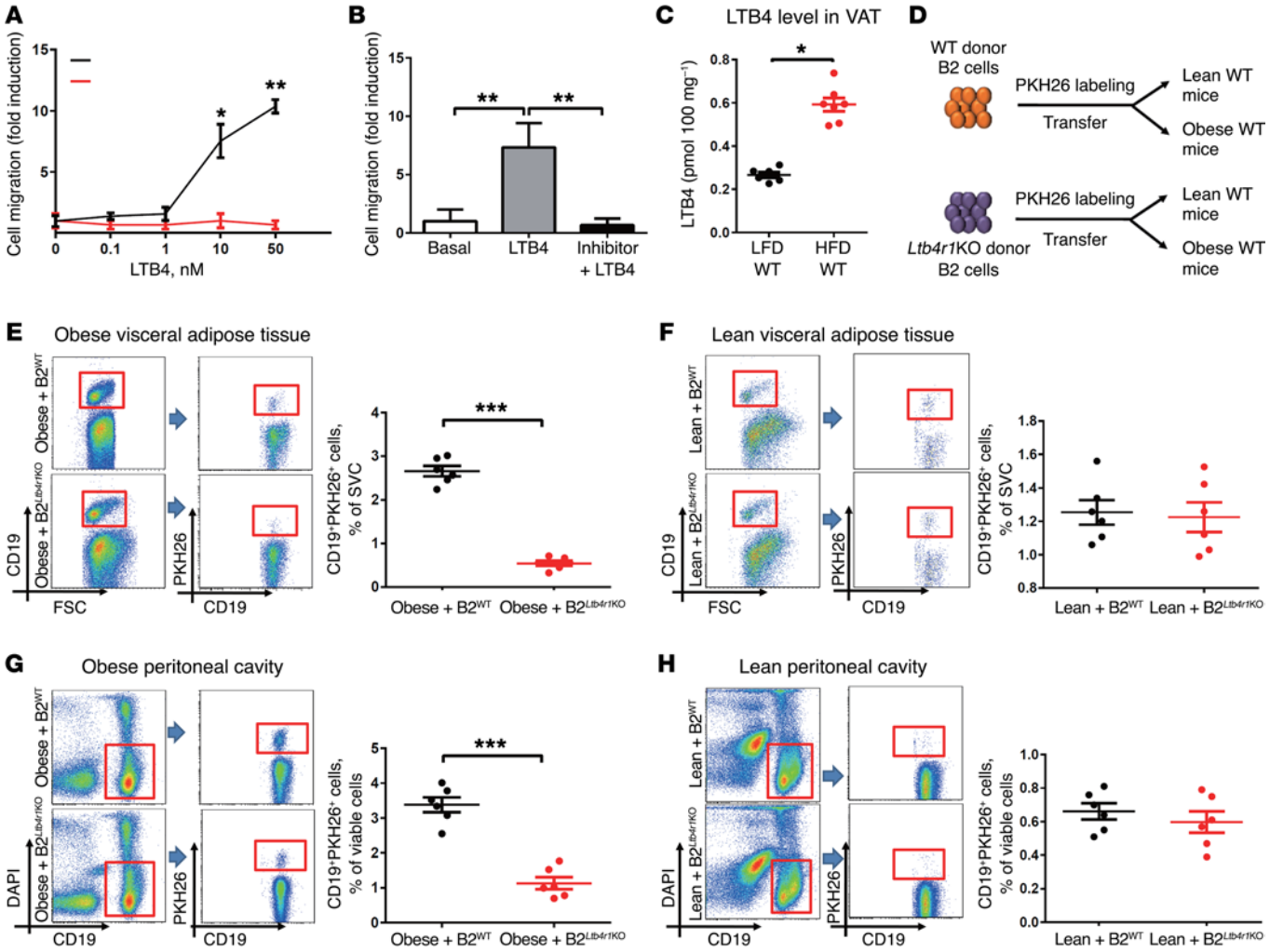

Figure 2. *Ltb4r1*KO blunts LTB4-mediated B2 cell chemotaxis both in vitro and in vivo. (**A**) In vitro B2 cell chemotaxis in response to LTB4 treatment. (**B**) Effect of LTB4R1 inhibitor (100 nM) on LTB4-mediated (50 nM) B2 cell chemotaxis. (**C**) LTB4 concentration in VAT of LFD- and HFD-fed WT mice. (**D**) Schematic diagram illustrating in vivo tracking of PKH26-labeled WT and *Ltb4r1*KO donor B2 cells in WT recipient mice. Recruitment of $CD19^+PKH26^+$ cells into VAT (**E** and **F**) and peritoneal cavity (**G** and **H**) of WT obese and lean recipient mice. Data are presented as mean ± SEM. n = 6-8 per group (**A**–**C**); n = 6 per group (**E**–**H**). $^*P < 0.05$, $^{**}P < 0.01$, $^{***}P < 0.001$, Student's t test (**A**, **C**, **E**–**H**); 1-way ANOVA with Bonferroni's post test (**B**).

To test the role of LTB4 and LTB4R1 on ATB2 cell recruitment in vivo, WT splenic B2 cells were labeled with the fluorescent dye PKH26 and transferred to either lean or obese WT recipient mice via i.v. injection (Figure 2D). After 5 days of adoptive transfer, PKH26-labeled B2 cells were quantified in the recipient mice using flow cytometric analyses. Consistent with the increased LTB4 levels in the obese recipients, we found a robust increase in $PKH26^+CD19^+$ B2 cells recruited into the VAT or peritoneal cavity of obese WT recipient mice compared with lean WT recipient mice (Figure 2, E–H). Interestingly, the number of PKH26-labeled *Ltb4r1*KO B2 cells tracking to the VAT or peritoneal cavity of obese WT recipient mice was much lower than in WT B2 cells (Figure 2, E and G). In the lean recipient mice with low tissue LTB4 levels, ATB2 cell content was minimal and the LTB4R1 knockout did not affect recruitment of $PKH26^+$ WT B2 cells (Figure 2, F and H). Taken together, these in vitro and in vivo results demonstrate that the LTB4/LTB4R1 axis exerts substantial effects on B2 cell recruitment during obesity.

Loss of LTB4R1 impairs obesity-induced B2 cell recruitment into adipose tissue. Given the role of LTB4R1 in LTB4-induced B2 cell recruitment, we next measured B2 cell accumulation in obese WT and *Ltb4r1*KO mice. The $CD19^+CD5^-$ B2 cell population in the spleen and peripheral circulation of HFD-fed *Ltb4r1*KO mice was comparable to that of HFD-fed WT mice (Figure 3, A and B). However, knockout of *Ltb4r1* led to a marked reduction in accumulation of B2 cells in VAT of obese mice, as shown by flow cytometry and immunohistochemistry staining (Figure 3, C and D). Consistent with our recent studies, the HFD-fed *Ltb4r1*KO mice displayed increased glucose tolerance and insulin sensitivity compared with obese WT mice (Supplemental Figure 3). Therefore, these results suggest that the reduction in B2 cell recruitment to VAT may be an important contributor to the improved insulin sensitivity seen in obese *Ltb4r1*KO mice.

The effects of B2 cells in inducing glucose intolerance and insulin resistance are LTB4R1 dependent. To further explore the importance of B2 cells and LTB4R1 in the pathogenesis of tissue inflammation

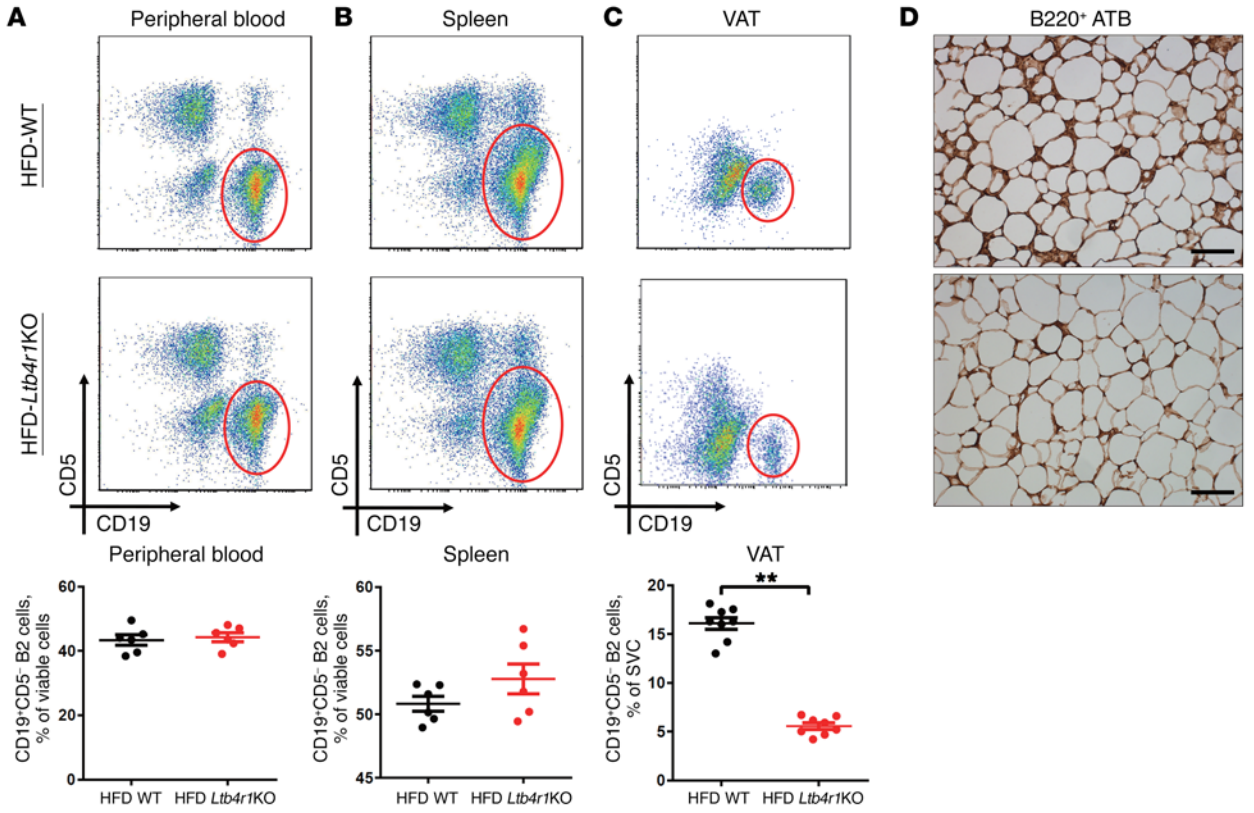

Figure 3. Ltb4r1KO mice exhibit reduced B2 cell accumulation in VAT during obesity. The population of $CD19^+CD5^-$ B2 cells in the peripheral blood (**A**), spleen (**B**), and VAT (**C**) of WT and *Ltb4r1*KO mice fed HFD for 12 weeks. (**D**) $B220^+$ B cells in VAT (ATB) of HFD-fed WT and *Ltb4r1*KO mice detected by immunostaining analysis. Scale bar: 100 μm. (**D**) Representative images shown from 4 independent experiments. Data are presented as mean ± SEM. n = 6–8 per group (**A**–**C**). $^{**}P < 0.01$, Student's t test.

and insulin resistance, WT ATB2 cells or *Ltb4r1*KO ATB2 cells were isolated from HFD mice by flow cytometry. The ATB2 cells (4×10^6) were then adoptively transferred into 10-week-old HFD B^{null} recipient mice. Body weight gain and food intake were monitored 2 weeks after transfer, and no differences were observed between the obese B^{null} recipient groups (Supplemental Figure 4, A and B). After 2 weeks, the obese B^{null} recipient mice engrafted with WT ATB2 cells (referred to as B^{null}/WT ATB2 mice) showed substantial glucose and insulin intolerance compared with obese/HFD control B^{null} mice (Figure 4, A and B). In contrast, obese B^{null} recipient mice adoptively transferred with *Ltb4r1*KO ATB2 cells (referred to as B^{null}/*Ltb4r1*KO ATB2 mice) did not develop glucose or insulin intolerance and maintained levels comparable to those of the control B^{null} mice (Figure 4, A and B). Insulin levels were similar between these obese B^{null} recipient mice (Supplemental Figure 4C). We also observed increased adipose tissue production of proinflammatory cytokines including *Tnfa*, *Il1b*, and *Il6* in B^{null}/WT ATB2 mice compared with control B^{null} or B^{null}/*Ltb4r1*KO ATB2 mice (Figure 4, C and D). This elevated inflammatory response was confirmed by finding increased activation of NF-κB signaling in the fat pads of obese B^{null}/WT ATB2 mice (Figure 4E).

In addition, insulin-stimulated adipose tissue Akt phosphorylation was decreased in B^{null}/WT ATB2 mice compared with control B^{null} mice, with no significant change in B^{null}/*Ltb4r1*KO ATB2 mice (Figure 4F). Since B2 cell adoptive transfer clearly confers systemic glucose intolerance and insulin resistance, we also examined insulin signaling in liver and muscle. As seen in Supplemental Figure 5, insulin-stimulated AKT phosphorylation was decreased in both of these tissues, comparable to the effects in adipose tissue, consistent with the systemic insulin-resistant state. Collectively, these results suggest that the LTB4/LTB4R1 axis regulates B2 cell recruitment in adipose tissue, contributing to the development of obesity-associated tissue inflammation and insulin resistance.

Flow cytometry analysis also identified marked differences in adipose tissue immune cell populations in B^{null}/WT ATB2 mice versus B^{null}/*Ltb4r1*KO ATB2 mice. Transfer of WT ATB2 cells led to a marked increase in total VAT $CD45^+CD19^+$ B cells compared with control B^{null} mice (Figure 4G). In contrast, *Ltb4r1*KO ATB2 cell transfer led to a much smaller increase in the VAT $CD45^+CD19^+$ B cell population (Figure 4G). In addition, transference of WT B2 cells led to an increased number of type 1 Th cells (Th1; IFN-γ^+CD4^+) with no change in Th2 (IL-4^+CD4^+) or Tregs ($Foxp3^+CD4^+$) in the VAT (Figure 4H). IFN-γ^+CD8^+ T cells were also increased in the B^{null}/WT ATB2 mice (Figure 4I). Finally, WT ATB2 cell transfer led to an increase in M1-like macrophages ($CD11b^+F4/80^+CD11c^+CD206^-$ cells) in VAT compared with control mice (Figure 4J). In contrast, adoptive transfer of *Ltb4r1*KO ATB2 cells into B^{null} mice was without effect on VAT T cell or macrophage populations (Figure 4J).

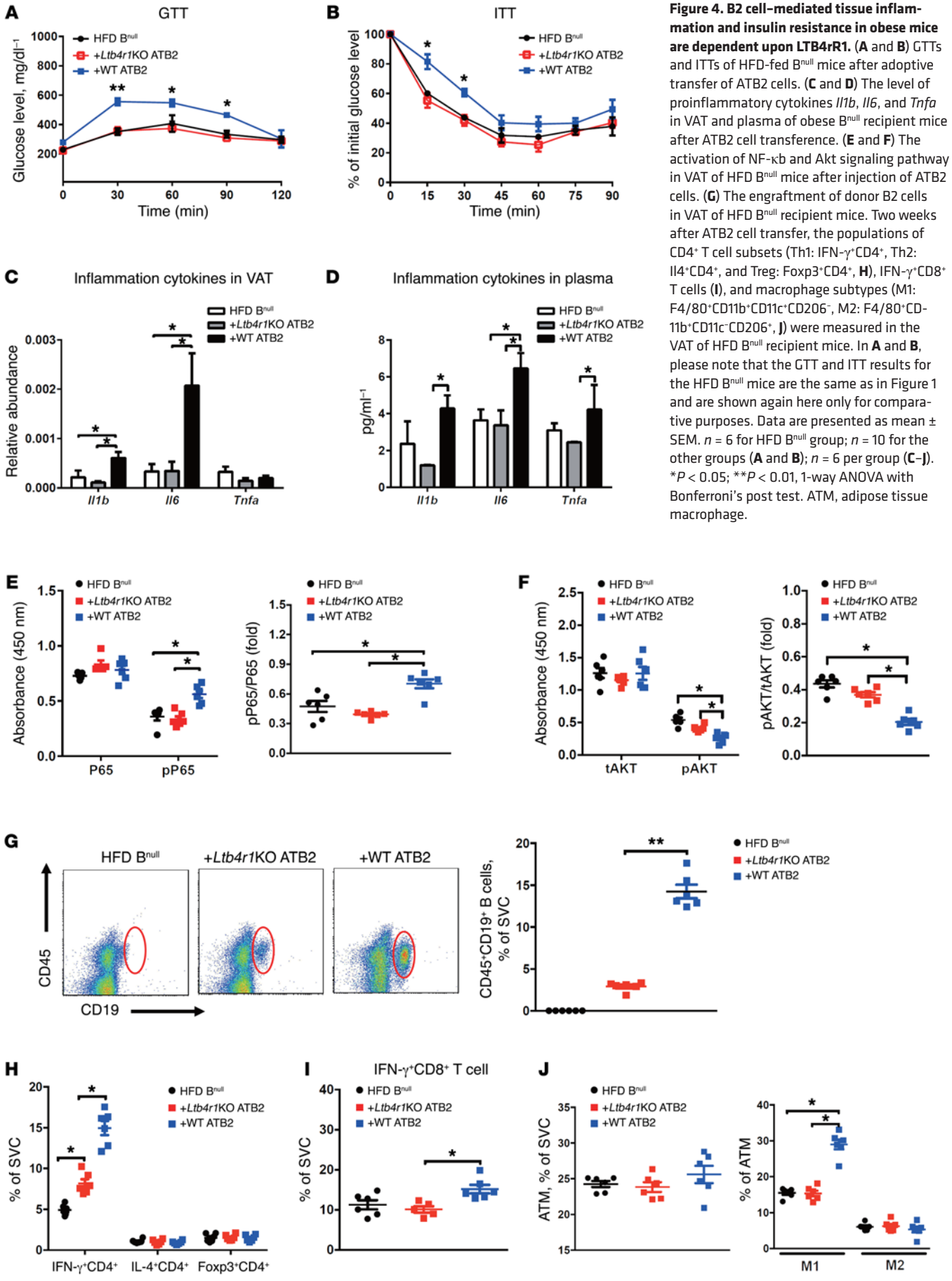

Figure 4. B2 cell–mediated tissue inflammation and insulin resistance in obese mice are dependent upon LTB4rR1. (**A** and **B**) GTTs and ITTs of HFD-fed B^{null} mice after adoptive transfer of ATB2 cells. (**C** and **D**) The level of proinflammatory cytokines *Il1b*, *Il6*, and *Tnfa* in VAT and plasma of obese B^{null} recipient mice after ATB2 cell transference. (**E** and **F**) The activation of NF-κb and Akt signaling pathway in VAT of HFD B^{null} mice after injection of ATB2 cells. (**G**) The engraftment of donor B2 cells in VAT of HFD B^{null} recipient mice. Two weeks after ATB2 cell transfer, the populations of CD4$^+$ T cell subsets (Th1: IFN-γ$^+$CD4$^+$, Th2: Il4$^+$CD4$^+$, and Treg: Foxp3$^+$CD4$^+$, **H**), IFN-γ$^+$CD8$^+$ T cells (**I**), and macrophage subtypes (M1: F4/80$^+$CD11b$^+$CD11c$^+$CD206$^-$, M2: F4/80$^+$CD-11b$^+$CD11c$^-$CD206$^+$, **J**) were measured in the VAT of HFD B^{null} recipient mice. In **A** and **B**, please note that the GTT and ITT results for the HFD B^{null} mice are the same as in Figure 1 and are shown again here only for comparative purposes. Data are presented as mean ± SEM. $n = 6$ for HFD B^{null} group; $n = 10$ for the other groups (**A** and **B**); $n = 6$ per group (**C**–**J**). $^*P < 0.05$; $^{**}P < 0.01$, 1-way ANOVA with Bonferroni's post test. ATM, adipose tissue macrophage.

Metabolic effects of ATB2 cells are partially dependent upon T cells and macrophages. B2 cells can act by modulating the recruitment or activation of adipose tissue macrophages and/or T cells. In an effort to deconvolute the metabolic consequences of B2 cell interactions with either macrophages or T cells, we pretreated HFD B^{null}, HFD B^{null}/WT ATB2, or HFD B^{null}/*Ltb4r1*KO ATB2 mice with either clodronate or anti-CD4/CD8 antibodies prior to adoptive transfer. The rationale was that clodronate leads to depletion of macrophages, whereas antibody treatment causes depletion of $CD4^+CD8^+$ T cells (Supplemental Figure 6) (38–41). Antibody-mediated T cell depletion in HFD B^{null} mice led to an improvement in glucose tolerance as well as insulin sensitivity (Figure 5A). This indicates an important effect of T cells on glucose and insulin metabolism in the complete absence of B cells. In the clodronate-treated HFD B^{null} mice, there was an even greater improvement in glucose and insulin tolerance, and this effect was the same whether or not clodronate was given in combination with anti–T cell antibodies (Figure 5A). Basal free fatty acid (FFA) levels were reduced, and acute insulin suppression of FFA levels was increased after clodronate or clodronate plus antibody treatment (Supplemental Figure 7). This is consistent with a robust effect of macrophages in inducing glucose intolerance and decreased insulin sensitivity in obesity and suggests that such effects are, at least partially, independent of B cells or T cells.

In the HFD B^{null}/WT ATB2 mice, antibody-mediated $CD4^+CD8^+$ T cell depletion prevented the increase in both glucose and insulin intolerance, with posttreatment values comparable to the responses seen in untreated control HFD B^{null} mice (Figure 5B). These data indicate that the systemic metabolic effects of B2 cells are, at least in part, dependent on downstream effector T cells. Clodronate-mediated depletion of macrophages in HFD B^{null}/WT ATB2 mice had an even greater effect in improving glucose and insulin tolerance, leading to glucose levels that were lower than those in control B^{null} mice (Figure 5B). Finally, as was seen with the B^{null} mice in Figure 5B, the combination of antibodies and clodronate treatment had an effect comparable to that of clodronate alone in improving glucose and insulin tolerance. This suggests that the adverse effects of B2 cells on glucose metabolism are partially dependent on macrophages, but that macrophages contribute to glucose and insulin intolerance through additional mechanisms that are B2 cell and T cell independent.

In these studies, we measured the content of adoptively transferred ATB2 cells in adipose tissues after antibody and/or clodronate treatment (Supplemental Figure 8). Interestingly, ATB2 cell accumulation after depletion of either $CD4^+CD8^+$ cells or macrophages was comparable to that seen in WT HFD mice (Figure 3C). These data suggest that these immune cell types are not a major source of the LTB4, which recruits B2 cells into the adipose tissue. This is consistent with the data in Supplemental Figure 2, which shows that primary adipocytes secrete significant amounts of LTB4, while SVCs produce very little. Taken together, these results suggest that adipocytes are a key source of the LTB4-mediated B2 cell recruitment into adipose tissue.

When these treatments were applied to the B^{null}/*Ltb4r1*KO ATB2 mice, since only a small number of *Ltb4r1*KO ATB2 cells appear in adipose tissue in these animals (Figure 4G), depletion of T cells (CD4/CD8 antibody) or macrophages (clodronate treatment) or a combination of the two led to the same glucose tolerance test (GTT) and insulin tolerance test (ITT) results as seen in untreated B^{null} mice (Supplemental Figure 9).

Consistent with the in vivo results on glucose and insulin tolerance, CD4/CD8 antibodies and clodronate treatment had marked effects in reducing adipose tissue inflammatory signaling and Akt phosphorylation in B^{null}/WT ATB2 mice, with much smaller effects in B^{null}/*Ltb4r1*KO ATB2 adipose tissue (Supplemental Figure 10).

In vitro B2 cell interactions with T cells and macrophages. To more directly assess the role of B2 cells in T cell activation, we incubated an equal number (0.1×10^6 cells) of ATB2 cells obtained from WT or *Ltb4r1*KO HFD/obese mice with WT splenic $CD4^+$ or $CD8^+$ T cells. Using this coculture method, we found that both WT and *Ltb4r1*KO ATB2s induced differentiation of both $CD4^+$ T cells and $CD8^+$ T cells into IFN-γ–expressing T cells, but the effect was substantially greater using the WT ATB2s (Figure 5C). These data are consistent with the in vivo results depicted in Figure 4, H and I, showing that adoptive transfer of WT ATB2 cells led to a greater increase in IFN-γ–expressing $CD4^+$ and $CD8^+$ cells in adipose tissue compared with *Ltb4r1*KO ATB2 cells.

With respect to macrophages, we cocultured WT ATB2s or *Ltb4r1*KO ATB2s with WT BM-derived macrophages (BMDMs) that had been stimulated with either LPS or IL-4/IL-13 to produce an M1-like or M2-like polarization state, respectively (42, 43). WT ATB2s had a greater effect in stimulating CD69 expression in M1-like BMDMs compared with *Ltb4r1*KO ATB2s (Figure 5D) accompanied by greater production of the proinflammatory cytokines *Tnfa*, *Il6*, and *Il1b* (Figure 5E). Interestingly, coculture of the WT or *Ltb4r1*KO ATB2s with M2-like BMDMs did not lead to a change in activation state (Supplemental Figure 11).

The LTB4/LTB4R1 axis promotes B2 cell activation. To examine the role of LTB4 on B2 cell activation, splenic B2 cells were stimulated with LPS (20 μg ml^{-1}) with or without LTB4 (100 nM). LPS-stimulated WT B2 cells exhibited an increased production of the proinflammatory cytokines *Ifng* and *Il6* compared with nonstimulated WT B2 cells (Supplemental Figure 12). These proinflammatory stimulatory characteristics were also observed when measuring phosphorylation of P65 (Figure 6C). LTB4 cotreatment further enhanced inflammatory signaling in the presence of LPS, as measured by proinflammatory cytokine production and activation of the NF-κB signaling pathway (Figure 6, A and C). In contrast, these LTB4 effects were absent in the *Ltb4r1*KO B2 cells (Figure 6, B and D).

Since LTB4R1 can be coupled to Gαi to mediate downstream signaling, we tested the effects of gain and loss of Gαi function on B2 cell responses. Pretreatment of WT B2 cells with the Gαi antagonist pertussis toxin (PT) (200 ng ml^{-1}) (34, 44, 45) inhibited LPS+LTB4-stimulated proinflammatory cytokine production and NF-κB activation (Figure 6, A and C), but was without effect in *Ltb4r1*KO B2 cells. Conversely, when WT B2 cells were pretreated with the Gαi agonist melittin (Mel) (1 μM) (46), there was an increase in the level of proinflammatory responses to both LPS and LTB4 (Figure 6, A and C). We next tested whether Mel could rescue the impaired inflammatory responses in the *Ltb4r1*KO B2 cells. Interestingly, Mel treatment markedly increased production of the proinflammatory cytokines *Ifng*, *Il1b*, and *Il6* in the *Ltb4r1*KO B2 cells in response to LPS and LTB4 (Figure 6B).

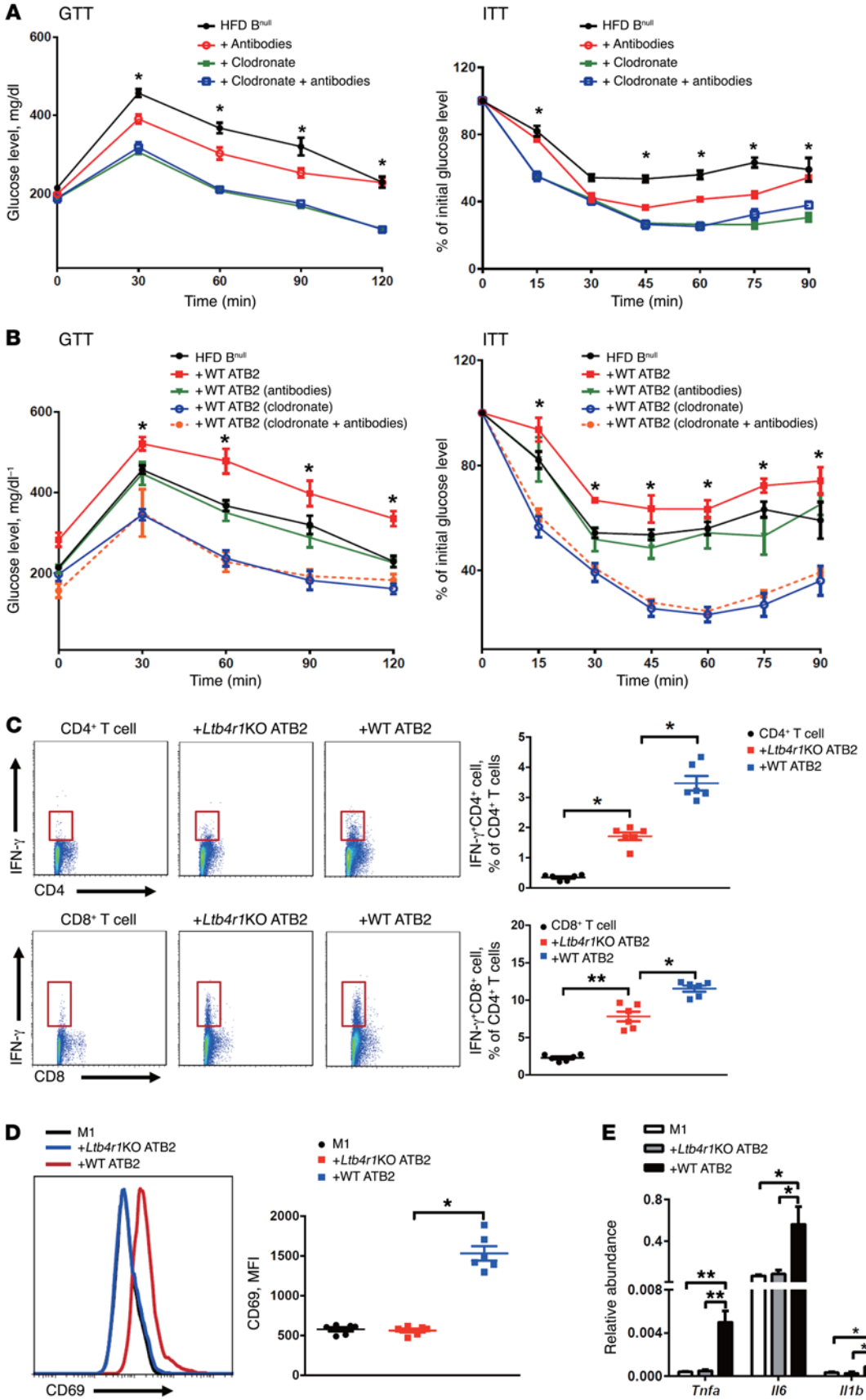

Figure 5. The mechanisms of ATB2 cells on insulin resistance and the role of LTB4R1 in this process. (**A**) GTTs and ITTs of HFD-fed B^{null} mice treated with T cell–depleting antibodies, macrophage-depleting clodronate, or both. (**B**) Two weeks after ATB2 cell transfer, GTT and ITT of HFD-fed B^{null} mice pretreated with clodronate or antibodies. (**C**) Differentiation of IFN-γ$^+$CD4$^+$ and IFN-γ$^+$CD8$^+$ T cells after coculture with WT or *Ltb4r1*KO ATB2 cells (WT ATB2, *Ltb4r1*KO ATB2), measured by flow cytometry analysis. (**D** and **E**) Levels of the cell surface marker CD69 and gene expression of the proinflammatory cytokines *Tnfa*, *Il6*, and *Il1b* in M1 macrophages after coculture with WT or *Ltb4r1*KO ATB2 cells. Data are presented as mean ± SEM. n = 8 per group (**A** and **B**); n = 6 per group (**C**–**E**). $^*P < 0.05$; $^{**}P < 0.01$, 1-way ANOVA with Bonferroni's post test.

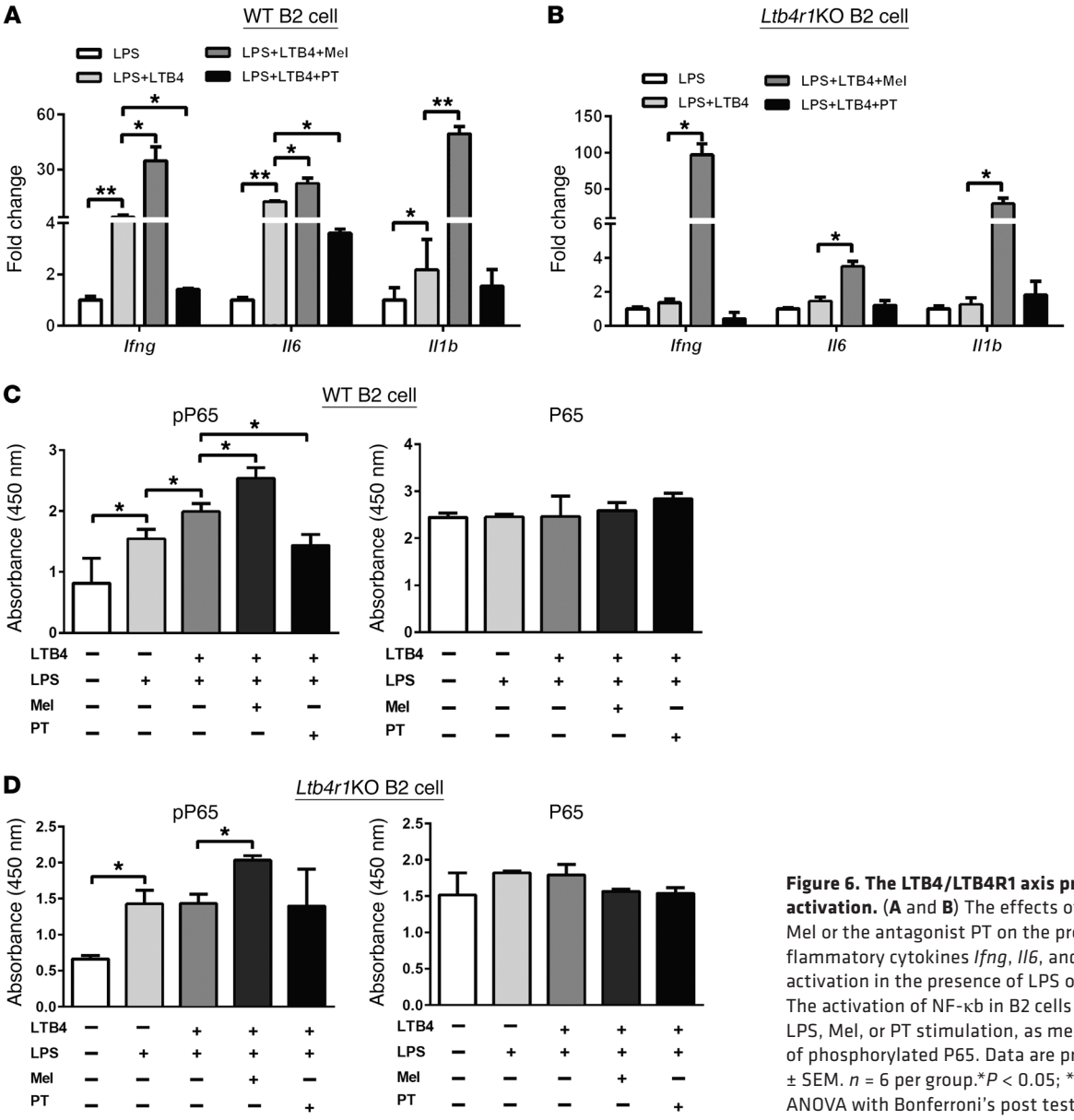

Figure 6. The LTB4/LTB4R1 axis promotes B2 cell activation. (**A** and **B**) The effects of the Gαi agonist Mel or the antagonist PT on the production of proinflammatory cytokines *Ifng*, *Il6*, and *Il1b* during B2 cell activation in the presence of LPS or LTB4. (**C** and **D**) The activation of NF-κb in B2 cells in response to LTB4, LPS, Mel, or PT stimulation, as measured by levels of phosphorylated P65. Data are presented as mean ± SEM. $n = 6$ per group.*$P < 0.05$; **$P < 0.01$, 1-way ANOVA with Bonferroni's post test.

Discussion

Chronic tissue inflammation, particularly in adipose tissue and liver, plays an important role in obesity-induced insulin resistance and glucose intolerance (7–11). There is clearly a complex interplay between the various immune cell types that orchestrates the inflammation-induced reduction in insulin sensitivity (47). Here, we show that obesity leads to the accumulation of B2 cells in adipose tissue and that these cells can coordinate insulin resistance through Th1 lymphocyte– and M1 macrophage–mediated mechanisms. Furthermore, these studies illustrate the role of LTB4 and its receptor, LTB4R1, on B2 cells in facilitating these processes. Thus, LTB4 recruits B2 cells to adipose tissue and also directly stimulates the B2 cell proinflammatory phenotype. In turn, the ATB2 cells then promote the proinflammatory activation state of Th1 lymphocytes and macrophages.

It is evident that B2 lymphocytes, various T cell subsets, and macrophages all accumulate in adipose tissue, liver, and possibly muscle as a consequence of obesity (14, 17, 19, 48–50). There are many levels of communication between these cell types that can regulate chemotaxis, tissue retention, and activation state (47). Clearly, stromal cells such as adipocytes, hepatocytes, and myocytes are key contributors to insulin resistance. In addition, within adipose tissue, liver, and muscle, there are other stromal cell types, such as endothelial cells and fibroblasts, and the possible impact of these cells on metabolic status remains to be better defined. Here, we show that B2 cells specifically participate in this process and that the number of activated B2 cells increases in adipose tissue in obesity, promoting the proinflammatory, insulin resistant, and glucose-intolerant state. B^{null} mice are a well-described model in which all B cell subtypes have been deleted (36). When B^{null} mice are placed on a HFD, the development of insulin resistance and glucose intolerance is mitigated compared with WT mice, indicating the importance of B cells in these processes. Adoptive transfer of ATB2 cells from WT HFD donor mice into HFD B^{null} recipient

mice promotes insulin resistance and glucose intolerance to the same extent as seen in HFD WT mice. This demonstrates the role of ATB2 cells in propagating the obesity-induced inflammatory/insulin-resistant state.

We found that ATB2 cells can directly activate $CD4^+$ and $CD8^+$ lymphocytes in a coculture setting and also activate macrophages toward an M1-like polarization state. When we conducted similar studies with *Ltb4r1*KO ATB2 cells, we found the deletion of LTB4R1 had a marked effect in attenuating the influence of ATB2 cells on T cell or macrophage activation. We further tested these concepts in vivo and found that depletion of $CD4^+CD8^+$ lymphocytes with an anti-CD4/CD8 antibody blocks the effect of ATB2s in causing insulin resistance and glucose intolerance. Interestingly, in vivo administration of clodronate to deplete macrophages also reversed insulin resistance and glucose intolerance. However, with macrophage depletion, the reversal is more profound, leading to an even greater state of insulin sensitivity and glucose tolerance than in HFD B^{null} mice, resulting in values similar to those seen in chow-fed WT mice. These results suggest that the effects of ATB2s in causing insulin resistance/glucose intolerance are partly dependent on T cells and macrophages. However, the large beneficial effect observed with clodronate treatment indicates that a sizeable component of the macrophage effect is independent of B and T cells. This suggests that in the context of chronic tissue inflammation, macrophages may be the final effector cells that directly cause dysregulated metabolism.

It is known that B cells can accumulate in obese adipose tissue (19–21), as shown in Figure 3D, but little is known about the mechanisms underlying their recruitment. Earlier work has shown that LTB4 can activate its receptor, LTB4R1, on macrophages to induce potent chemotactic effects (31, 34). In the current studies, we show that LTB4 levels are elevated in adipose tissue from obese mice and that there is increased expression of LTB4R1 on ATB2 cells obtained from obese animals. Based on this, we hypothesized that the LTB4/LTB4R1 axis could provide a key function leading to the increased content of ATB2 cells in obesity. Consistent with this idea, our data show that LTB4 has robust effects to stimulate chemotaxis of B2 cells in vitro. In addition, in vivo B2 cell tracking studies demonstrate that when fluorescently labeled B2 cells are injected into lean or obese recipient mice, much greater numbers of B2 cells appear in obese adipose tissue compared with tissue in lean mice. In contrast, when fluorescently labeled *Ltb4r1*KO B2 cells were injected, the migration of these cells to adipose tissue and the peritoneal cavity was markedly impaired compared with WT B2 cells. Taken together, these results indicate that, in obesity, tissue levels of LTB4 play an important role in attracting B2 cells to their pathophysiologic sites of action. In addition, treatment of WT B2 cells with LTB4 stimulates WT B2 cell proinflammatory cytokine expression as well as P65 activation. These effects are additive to those of LPS. In contrast, LTB4 was without these proinflammatory stimulatory effects in *Ltb4r1*KO B2 cells. Thus, LTB4 can promote the interaction between B2 cells and T cells or macrophages. In this way, LTB4/LTB4R1 serves as a control point regulating ATB2 cell content as well as the subsequent effect of B2 cells in promoting the proinflammatory state of other immune cell types.

Previous studies have shown that B cells might contribute to obesity-induced inflammation and that human B cells have similar properties (19–21). However, the specific B cell subtype responsible has not been previously assessed. In addition, while an earlier study indicated that pathogenic antibodies elaborated by B cells can cause insulin resistance, two earlier reports have failed to confirm effects of B cell antibodies in causing impaired insulin sensitivity (20, 21). Our current studies contain no specific experiments related to such antibodies. In this paper, we focus on several additional B cell–related mechanisms. For example, we demonstrate that it is the B2 subset that specifically causes metabolic dysfunction. Furthermore, we also demonstrate the importance of the LTB4/LTB4R1 axis in mediating ATB2 cell recruitment and activation. Our data also provide evidence, both in vitro and in vivo, that ATB2 cells can induce inflammation/insulin resistance through downstream effector T cells and macrophages. Interestingly, we found increased accumulation of adoptively transferred B2 cells in obese adipose tissue, even after depletion of T cells and/or macrophages. These data indicate that these immune cell types are not the major source of the adipose tissue LTB4, which recruits B2 cells. This also fits with our results showing that SVCs produced only small amounts of LTB4 compared with adipocytes (Supplemental Figure 2).

In these studies, we have shown that B2 lymphocytes accumulate in adipose tissue as a result of obesity and that these cells directly contribute to inflammation, insulin resistance, and glucose intolerance. The LTB4/LTB4R1 chemokine system provides a key signal for recruiting B2 cells to the adipose tissue. Several different immune cell types are present in obese adipose tissue composing a complex intercellular communication network. Here, we show that ATB2 cells can activate T cells and macrophages in adipose tissue and that the effects of ATB2 cells in causing insulin resistance are dependent on T cells, with a partial dependency on ATMs. These results highlight the importance of B2 cells and the communication system between adipose tissue immune cell types in the pathophysiology of inflammation/insulin resistance and suggest that inhibition of LTB4R1 could be a useful approach in insulin-sensitizing therapeutics.

Methods

Animal care and use. The generation of B^{null} and *Ltb4r1*KO mice has been previously described (34, 36). All mice were maintained on a 12-hour light/12-hour dark cycle. Male mice 5 to 6 weeks of age were fed ad libitum. Mice were fed a HFD (60% fat calories, 20% protein calories, and 20% carbohydrate calories; Research Diets) or a LFD (10% fat calories, 20% protein calories, and 70% carbohydrate calories; Research Diets).

Isolation of stromal cells from VATs. VAT was mechanically chopped and then digested with collagenase II for 15 minutes at 37°C. After passing cells through a 100-μm cell strainer and centrifugation at 1,000 *g* for 10 minutes, primary adipocytes were collected from the top layer of the supernatant and the pellet containing the SVC fraction was then incubated with red blood cell lysis buffer.

Immune cell isolation analysis. For the in vitro and in vivo B2 cell chemotaxis assays, B2 cells were isolated from spleen of LFD-fed WT or *Ltb4r1*KO mice. For the B2 cell adoptive transfer assay in HFD B^{null} mice, B2 cells were isolated from VAT of HFD-fed (for 12 weeks) WT or *Ltb4r1*KO mice. T cells were isolated from spleen of LFD-fed WT mice and used for coculture assays. Single cell suspensions were incubated

with fluorescence-tagged antibodies against CD4 or CD8 for T cells, or CD19 or CD5 for B cells. $CD4^+$ T cells, $CD8^+$ T cells, $CD19^+CD5^+$ B1 cells, and $CD19^+CD5^-$ B2 cells were purified using BD FACS Aria II flow cytometer (BD Biosciences). BMDMs were prepared as previously described (42, 43).

Immune cell activation analysis. For B2 cell activation assays, B2 cells were stimulated with LPS (20 μg ml^{-1}) (21). For macrophage polarization analysis, BMDMs were stimulated with LPS (100 ng ml^{-1}) for M1 or IL-4 and IL-13 (20 ng ml^{-1} of each) for M2-polarized activation (42, 43). T cells were activated by anti-CD3 and anti-CD28 precoated on a cell culture plate.

Coculture assay. ATB2 cells (0.1×10^6) isolated from HFD-fed WT or *Ltb4r1*KO mice were mixed with WT splenic $CD4^+$ or $CD8^+$ T cells at a ratio of 1:1 in the presence of CD3 and CD28. WT or *Ltb4r1*KO ATB2 cells (0.1×10^6/well) were also cocultured with WT M1 or M2 BMDMs at a ratio of 1:2 using a Transwell plate (0.4 μm polycarbonate filter, Corning), with BMDMs placed in the lower chamber and ATB2 cells in the upper chamber. The activation of BMDMs or T cells was examined by flow cytometry with antibodies against CD69 or IFN-γ after 72 hours of coculture. The gene expression of proinflammatory cytokines *Tnfa*, *Il6*, and *Il1b* or antiinflammatory cytokine *Il10* was measured by quantitative PCR (qPCR).

In vitro chemotaxis assay. In vitro chemotaxis assays were performed as previously described (34, 37). Briefly, ATB2 cells isolated from either HFD-fed WT or *Ltb4r1*KO mice were placed in the upper chamber of a 5-μm polycarbonate filter, and RPMI with or without LTB4 (Cayman Chemical) was placed in the lower chamber. After 3 hours of migration at 37°C, cells in the lower chamber were collected and counted.

In vivo B2 cell tracking. ATB2 cells isolated from HFD-fed WT or *Ltb4r1*KO mice were washed in serum-free RPMI 1640 and suspended in PKH26 labeling buffer (containing 2×10^{-3} M PKH26; Sigma-Aldrich) (34). After 10 minutes incubation in the dark, the PKH26-labeling assay was stopped by adding an equal volume of medium supplemented with 10% FBS. The PKH26-labled B2 cells (1×10^6) were adoptively transferred into each LFD- or HFD-fed WT recipient mouse via i.v. injection. Five days after injection, recipient mice were sacrificed, tissues harvested, and the presence of PKH26-labeled B2 cells in the peritoneal cavity and VAT was examined by FACS.

Adoptive transfer of B2 cells. A total of 4×10^6 ATB2 cells in 100 μl of PBS were transferred into HFD-fed (for 8 weeks) B^{null} mice via i.v. injection. HFD B^{null} mice without B2 cell transfer served as controls. Glucose tolerance and insulin sensitivity were determined 2 weeks after the B cell injection.

GTTs and ITTs. For GTTs, mice received 1 dose of dextrose (1 g kg^{-1} body weight) via i.p. injection after 6 hours of fasting. For ITTs, mice were fasted for 6 hours and then i.p. injected with insulin (0.70 units/kg^{-1} body weight).

Flow cytometry analysis. Unless otherwise specified, we purchased antibodies from eBioscience. Visceral stromal cells or splenic cells were stained with fluorescence-tagged antibodies to detect cell lineages. B cell subtypes were detected with antibodies against CD19 (catalog 17-0193-82) and CD5 (catalog 11-0051-82); T cells were detected with antibodies against CD4 (catalog 17-0041-81), CD8 (catalog 12-0081-81), Foxp3 (catalog 11-5773-82), IFN-γ (catalog 25-7311-82), and IL-4 (catalog 53-7041-80); macrophage subtypes were detected with antibodies against F4/80 (catalog 25-4801-82), CD11b (catalog 53-0112-80), CD206 (catalog 141706, BioLegend), and CD11c (catalog 12-0114-83). Macrophage activation was measured with antibodies against CD69 (catalog 48-0691-80). T cell activation was measured using antibodies against IFN-γ (catalog 25-7311-82). Data were analyzed using FlowJo software.

Multiplex protein expression assay. The plasma concentrations of IL-1b, TNF-α, and IL-6 were determined using MILLIPLEX Multiplex assays (EMD Millipore) on a MAGPIX instrument (EMD Millipore). Results were analyzed using xPONENT 4.2 software (EMD Millipore).

Immunohistochemistry. Tissues collected from HFD-fed mice were fixed in 4% paraformaldehyde, embedded in paraffin, and sectioned. Deparaffinized sections were stained with a rat anti-mouse antibody against B220 (catalog 550286, BD Biosciences) to detect B cells, followed by incubation with a biotinylated anti-rat secondary antibody (BD Biosciences). Slides were subsequently incubated with HRP-streptavidin (Jackson ImmunoResearch) and developed in substrate chromogen. Immunoglobulin protein was used as the negative control. Slides were counterstained with Mayer's and mounted with VectaShield mounting media. Images were captured using a NanoZoomer slide scanner system with NanoZoomer Digital Pathology software (Hamamatsu).

Tissue macrophage and T cell depletion studies. To deplete tissue macrophages, B^{null} mice fed for 8 weeks with HFD were given clodronate liposomes (80 mg kg^{-1} body weight; catalog F70101C-N, FormuMax) every 3 days via i.p. injection (34, 38, 39). After 6 days of clodronate treatment, B2 donor cells were transferred into these B^{null} mice. After transferring B2 donor cells, B^{null} recipient mice also received clodronate treatment (80 mg kg^{-1} body weight) every 5 days. HFD B^{null} mice treated with control liposome injections were used as control.

For T cell depletion, HFD B^{null} mice were i.p. injected with 20 μg of anti-CD4 (catalog 16-0041-86, eBiosciences) and 20 μg of anti-CD8 (catalog 16-0081-85, eBioscience) antibodies in 100 μl PBS for 4 consecutive days (40, 41). After adoptive transfer of B2 cells, B^{null} mice received antibody treatment every 3 days. HFD B^{null} mice injected with IgG were used as the control.

PT and Mel treatment. B2 cells were treated with the Gαi antagonist PT (catalog 516560, Calbiochem) at a dose of 200 ng ml^{-1} or the Gαi agonist Mel (catalog 20449-79-0, Sigma-Aldrich) at a concentration of 1 μM (34, 44–46).

LTB4, FFA, P65, and Akt measurements. The production of LTB4 in VAT or mature adipocytes and SVCs was measured by using an ELISA kit (catalog 520111, Cayman Chemical). The plasma FFA level was measured by using an ELISA kit (Wako Diagnostics). The tissue levels of pP65, total P65, pAkt, and total Akt were measured by using ELISA kits (eBioscience).

Statistics. Results are expressed as mean ± SEM. Each data point derived from qPCR assays represents an average of 2 technical replicates. The statistical significance of the differences between various treatments was measured by either the 2-tailed Student's *t* test or 1-way ANOVA with Bonferroni's post-test. Data analyses were performed using GraphPad Prism software version 6.0. A value of $P < 0.05$ was considered statistically significant.

Study approval. All animal procedures were reviewed and approved by the IACUC (Institutional Animal Care and Use Committee) of the University of California, San Diego and all animals were randomly assigned to cohorts when used.

Author contributions

WY designed the studies and performed most of the experiments. JW, GB, and PL assisted with the tissue collection. JW and PL assisted with in vitro cell chemotaxis assay. JM Ofrecio performed ELISA assays and genotyping. DEO and JW assisted with histology analysis. DYO assisted with in vivo B2 cell tracking assays. YSL assisted with clodronate assay. WY and JM Olefsky analyzed and interpreted the data, supervised the project, and cowrote the manuscript. WY, OO, and JM Olefsky revised the manuscript.

Acknowledgments

This study was funded by the American Heart Association (16POST31350039 to WY) and the US National Institute of Diabetes and Digestive and Kidney Diseases (DK033651, DK074868, DK063491, DK09062 to JM Olefsky).

Address correspondence to: Jerrold M. Olefsky, Stein Clinical Research Building, Room 227, Department of Medicine, Division of Endocrinology and Metabolism, University of California, San Diego, La Jolla, California 92093, USA. Phone: 858.534.6651; E-mail: jolefsky@ucsd.edu.

1. National Diabetes Statistics Report: Estimates of Diabetes and its Burden in the United States, 2014. Centers for Disease Control and Prevention. https://www.cdc.gov/diabetes/pubs/statsreport14/national-diabetes-report-web.pdf. Accessed December 29, 2016.
2. Flegal KM, Kruszon-Moran D, Carroll MD, Fryar CD, Ogden CL. Trends in Obesity Among Adults in the United States, 2005 to 2014. *JAMA*. 2016;315(21):2284–2291.
3. Wilson PW, D'Agostino RB, Parise H, Sullivan L, Meigs JB. Metabolic syndrome as a precursor of cardiovascular disease and type 2 diabetes mellitus. *Circulation*. 2005;112(20):3066–3072.
4. Romeo GR, Lee J, Shoelson SE. Metabolic syndrome, insulin resistance, and roles of inflammation--mechanisms and therapeutic targets. *Arterioscler Thromb Vasc Biol*. 2012;32(8):1771–1776.
5. Johnson AM, Olefsky JM. The origins and drivers of insulin resistance. *Cell*. 2013;152(4):673–684.
6. Kahn SE, Hull RL, Utzschneider KM. Mechanisms linking obesity to insulin resistance and type 2 diabetes. *Nature*. 2006;444(7121):840–846.
7. Holland WL, et al. Lipid-induced insulin resistance mediated by the proinflammatory receptor TLR4 requires saturated fatty acid-induced ceramide biosynthesis in mice. *J Clin Invest*. 2011;121(5):1858–1870.
8. Hotamisligil GS, Arner P, Caro JF, Atkinson RL, Spiegelman BM. Increased adipose tissue expression of tumor necrosis factor-alpha in human obesity and insulin resistance. *J Clin Invest*. 1995;95(5):2409–2415.
9. Xu H, et al. Chronic inflammation in fat plays a crucial role in the development of obesity-related insulin resistance. *J Clin Invest*. 2003;112(12):1821–1830.
10. Hotamisligil GS, Peraldi P, Budavari A, Ellis R, White MF, Spiegelman BM. IRS-1-mediated inhibition of insulin receptor tyrosine kinase activity in TNF-alpha- and obesity-induced insulin resistance. *Science*. 1996;271(5249):665–668.
11. Shoelson SE, Lee J, Yuan M. Inflammation and the IKK beta/I kappa B/NF-kappa B axis in obesity- and diet-induced insulin resistance. *Int J Obes Relat Metab Disord*. 2003;27 Suppl 3:S49–S52.
12. Lumeng CN, Deyoung SM, Bodzin JL, Saltiel AR. Increased inflammatory properties of adipose tissue macrophages recruited during diet-induced obesity. *Diabetes*. 2007;56(1):16–23.
13. Nishimura S, et al. CD8+ effector T cells contribute to macrophage recruitment and adipose tissue inflammation in obesity. *Nat Med*. 2009;15(8):914–920.
14. Winer S, et al. Normalization of obesity-associated insulin resistance through immunotherapy. *Nat Med*. 2009;15(8):921–929.
15. Morris DL, et al. Adipose tissue macrophages function as antigen-presenting cells and regulate adipose tissue CD4+ T cells in mice. *Diabetes*. 2013;62(8):2762–2772.
16. Cipolletta D, et al. PPAR-γ is a major driver of the accumulation and phenotype of adipose tissue Treg cells. *Nature*. 2012;486(7404):549–553.
17. Oh DY, Morinaga H, Talukdar S, Bae EJ, Olefsky JM. Increased macrophage migration into adipose tissue in obese mice. *Diabetes*. 2012;61(2):346–354.
18. Feuerer M, et al. Lean, but not obese, fat is enriched for a unique population of regulatory T cells that affect metabolic parameters. *Nat Med*. 2009;15(8):930–939.
19. Winer DA, et al. B cells promote insulin resistance through modulation of T cells and production of pathogenic IgG antibodies. *Nat Med*. 2011;17(5):610–617.
20. DeFuria J, et al. B cells promote inflammation in obesity and type 2 diabetes through regulation of T-cell function and an inflammatory cytokine profile. *Proc Natl Acad Sci USA*. 2013;110(13):5133–5138.
21. Ying W, et al. miR-150 regulates obesity-associated insulin resistance by controlling B cell functions. *Sci Rep*. 2016;6:20176.
22. Samuelsson B, Dahlén SE, Lindgren JA, Rouzer CA, Serhan CN. Leukotrienes and lipoxins: structures, biosynthesis, and biological effects. *Science*. 1987;237(4819):1171–1176.
23. Haeggström JZ. Leukotriene A4 hydrolase/aminopeptidase, the gatekeeper of chemotactic leukotriene B4 biosynthesis. *J Biol Chem*. 2004;279(49):50639–50642.
24. Tager AM, Luster AD. BLT1 and BLT2: the leukotriene B(4) receptors. *Prostaglandins Leukot Essent Fatty Acids*. 2003;69(2-3):123–134.
25. Goodarzi K, Goodarzi M, Tager AM, Luster AD, von Andrian UH. Leukotriene B4 and BLT1 control cytotoxic effector T cell recruitment to inflamed tissues. *Nat Immunol*. 2003;4(10):965–973.
26. Sánchez-Galán E, et al. Leukotriene B4 enhances the activity of nuclear factor-kappaB pathway through BLT1 and BLT2 receptors in atherosclerosis. *Cardiovasc Res*. 2009;81(1):216–225.
27. Yokomizo T, Izumi T, Chang K, Takuwa Y, Shimizu T. A G-protein-coupled receptor for leukotriene B4 that mediates chemotaxis. *Nature*. 1997;387(6633):620–624.
28. Huang L, et al. Leukotriene B4 strongly increases monocyte chemoattractant protein-1 in human monocytes. *Arterioscler Thromb Vasc Biol*. 2004;24(10):1783–1788.
29. Colom B, et al. Leukotriene B4-neutrophil elastase axis drives neutrophil reverse transendothelial cell migration in vivo. *Immunity*. 2015;42(6):1075–1086.
30. Horrillo R, et al. 5-lipoxygenase activating protein signals adipose tissue inflammation and lipid dysfunction in experimental obesity. *J Immunol*. 2010;184(7):3978–3987.
31. Spite M, et al. Deficiency of the leukotriene B4 receptor, BLT-1, protects against systemic insulin resistance in diet-induced obesity. *J Immunol*. 2011;187(4):1942–1949.
32. Bäck M, et al. Leukotriene production is increased in abdominal obesity. *PLoS One*. 2014;9(12):e104593.
33. Mothe-Satney I, et al. Adipocytes secrete leukotrienes: contribution to obesity-associated inflammation and insulin resistance in mice. *Diabetes*. 2012;61(9):2311–2319.
34. Li P, et al. LTB4 promotes insulin resistance in obese mice by acting on macrophages, hepatocytes and myocytes. *Nat Med*. 2015;21(3):239–247.
35. Sears DD, et al. Mechanisms of human insulin resistance and thiazolidinedione-mediated insulin sensitization. *Proc Natl Acad Sci USA*. 2009;106(44):18745–18750.
36. Kitamura D, Roes J, Kühn R, Rajewsky K. A B cell-deficient mouse by targeted disruption of the membrane exon of the immunoglobulin mu chain gene. *Nature*. 1991;350(6317):423–426.
37. Badr G, et al. BAFF enhances chemotaxis of primary human B cells: a particular synergy between BAFF and CXCL13 on memory B cells. *Blood*. 2008;111(5):2744–2754.
38. Weisser SB, van Rooijen N, Sly LM. Depletion and reconstitution of macrophages in mice. *J Vis Exp*. 2012;66(66):e4105.
39. van Rooijen N, Hendrikx E. Liposomes for specific depletion of macrophages from organs and tissues. *Methods Mol Biol*. 2010;605:189–203.
40. Loubaki L, Tremblay T, Bazin R. In vivo depletion of leukocytes and platelets following injection of T cell-specific antibodies into mice. *J Immunol Methods*. 2013;393(1-2):38–44.
41. Grcević D, Lee SK, Marusić A, Lorenzo JA. Depletion of CD4 and CD8 T lymphocytes in mice in vivo enhances 1,25-dihydroxyvitamin D3-stimulated osteoclast-like cell formation in vitro by a mechanism that is dependent on prostaglandin synthesis. *J Immunol*. 2000;165(8):4231–4238.
42. Ying W, Cheruku PS, Bazer FW, Safe SH, Zhou B.

Investigation of macrophage polarization using bone marrow derived macrophages. *J Vis Exp*. 2013;76(76):e50323.
43. Ying W, et al. MicroRNA-223 is a crucial mediator of PPARγ-regulated alternative macrophage activation. *J Clin Invest*. 2015;125(11):4149–4159.
44. Peres CM, Aronoff DM, Serezani CH, Flamand N, Faccioli LH, Peters-Golden M. Specific leukotriene receptors couple to distinct G proteins to effect stimulation of alveolar macrophage host defense functions. *J Immunol*. 2007;179(8):5454–5461.
45. Lee SP, Serezani CH, Medeiros AI, Ballinger MN, Peters-Golden M. Crosstalk between prostaglandin E2 and leukotriene B4 regulates phagocytosis in alveolar macrophages via combinatorial effects on cyclic AMP. *J Immunol*. 2009;182(1):530–537.
46. Aeffner F, Davis IC. Respiratory syncytial virus reverses airway hyperresponsiveness to methacholine in ovalbumin-sensitized mice. *PLoS One*. 2012;7(10):e46660.
47. Tsai S, Clemente-Casares X, Revelo XS, Winer S, Winer DA. Are obesity-related insulin resistance and type 2 diabetes autoimmune diseases? *Diabetes*. 2015;64(6):1886–1897.
48. Weisberg SP, McCann D, Desai M, Rosenbaum M, Leibel RL, Ferrante AW. Obesity is associated with macrophage accumulation in adipose tissue. *J Clin Invest*. 2003;112(12):1796–1808.
49. Kanda H, et al. MCP-1 contributes to macrophage infiltration into adipose tissue, insulin resistance, and hepatic steatosis in obesity. *J Clin Invest*. 2006;116(6):1494–1505.
50. Morinaga H, et al. Characterization of distinct subpopulations of hepatic macrophages in HFD/obese mice. *Diabetes*. 2015;64(4):1120–1130.